https://doi.org/10.31871/WJIR.12.6.13
World Journal of Innovative Research (WJIR)
ISSN: 2454-8236, Volume-12, Issue-6, June 2022 Pages 05-07

# Atmospheric Correction of SPOT Satellite Images

**Chien-Hui Liu**

***Abstract*—Atmospheric correction (AC) is an essential procedure to quantitatively analyze remote sensing data. Atmospheric effect (AE) of satellite images can be corrected to obtain surface reflectance from top-of-atmospheric signal. This study is to introduce the atmospheric correction method of SPOT satellite image. The results show that AC is important, especially at visible bands. Neglecting AC can lead relative errors of reflectance to 64% and 32% at green and red bands, respectively. The physical mechanism of AE at visible, near-IR and shortwave IR bands is also explained.**

***Index Terms*—Atmospheric Correction, Remote Sensing, SPOT Satellite, Surface Reflectance.**

## I. Introduction

Quantitative analysis of remote sensing data is usually hampered by atmospheric effect (AE) of satellite images [1]–[3]. Top-of-Atmosphere reflectance derived from remote sensing images is deviated from true surface reflectance due to the scattering and absorption of both molecules and aerosol. AE always brightens the dark targets and darkens the bright targets; thus, reduces the contrast of satellite imagery [1]. To correct AE and retrieve surface reflectance, atmospheric correction AC of satellite image is necessary.

Most widely used AC algorithm for satellite images is using dark target (DT) to retrieve surface reflectance [4]–[7]. Simple dark object subtraction is also based on DT [8]–[10]. Radiative transfer model can be used in AC of satellite image to retrieve true surface reflectance [5]. Aerosol optical depths (AODs) are derived from the Landsat TM scene itself using DT [11]–[13]. DT approach is also used in MODIS AC, accompanied with deep blue method [6], [14], [15]. Surface reflectance obtained by AC can be further applied in terrestrial monitoring using physical approaches, such as leaf area index (LAI) and fraction of photosynthetically active radiation (FPAR) absorbed by vegetation [16].

The objective of the paper is to introduce the atmospheric correction algorithm of SPOT satellite image. The atmospheric effect on the surface reflectance is analyzed. The physical mechanism of AE at visible, near-IR (NIR) and shortwave IR (SWIR) bands is explained.

## II. Atmospheric Correction Algorithm

### A. TOA Reflectance Modeling

If the surface is assumed to be uniform and Lambertian as well as gas absorption is neglected, a satellite sensor received TOA reflectance $\rho^{TOA}$ by a target reflectance $\rho$ at sea level altitude under solar and viewing zenith angles $\theta s$, $\theta v$ and relative azimuthal angle $\phi$ within narrow spectral bands can be written as [17]:

$$\rho^{TOA}(\mu_s,\mu_v,\phi)=\rho_a(\mu_s,\mu_v,\phi)+T(\mu_s)T(\mu_v)\frac{\rho}{1-\rho S} \quad (1)$$

where $\rho_a$ is the atmospheric reflectance; $\mu_s$ and $\mu_v$ are $\cos\theta_s$ and $\cos\theta_v$; $T(\mu_s)$ and $T(\mu_v)$ are the downward and upward total scattering transmittances, and $S$ is the spherical albedo of the atmosphere. Atmospheric functions, including $\rho_a$, $T(\mu_s)$, $T(\mu_v)$ and $S$, are all functions of AOD and aerosol models. Hence, $\rho^{TOA}$ also vary with aerosol properties, i.e. AOD and aerosol models, and $\rho$.

Simulations of $\rho^{TOA}$ through equation (1) rely on radiative transfer simulations using the vector version of Second Simulation of a Satellite Signal in the Solar Spectrum (6S), 6SV [17]. The accuracy of 6SV has been validated to be within 1% [17].

### B. Aerosol Optical Depth Retrieval

Before atmospheric correction of satellite remotely sensed data, aerosol optical depth (AOD) needs to be retrieved from image itself. Atmospheric effect is assumed to be uniform and with cloudless. AOD is retrieved using 6SV with darkest pixel (DP) at red band [18]. Feasible maritime aerosol model is considered. Darkest pixel at red band is assumed of reflectance of 0.01 as performed in previous study [18]. AOD can be obtained based on the 6SV run.

### C. Atmospheric Correction

Atmospheric correction of satellite image can retrieve surface reflectance from TOA reflectance. Based on the retrieved AOD, surface reflectance can be obtained from lookup table (LUT). LUT is pre-computed by multiple runs of 6SV for surface reflectance ranging from 0 to 1 by step of 0.01 [18]. Then surface reflectance can be obtained from TOA reflectance for every pixel.

## III. Results and Discussion

Fig. 1 shows raw image of SPOT satellite for Taoyuan test site. This image covers Zhongli city, Taoyuan and taken on 2010/03/11. As one can see, whole area covers mainly with vegetation and urban area covers on the right side of the image as well as water ponds (dark) scattered around the area.

Histogram of TOA reflectance and surface reflectance at green band is shown in Fig. 2. Since atmospheric scattering is dominated at visible bands, such as green and red bands, surface reflectance is greatly reduced when AC is performed. Fig. 3 also shows that the error of TOA reflectance is positive for the whole image. The error of TOA reflectance due to neglection of AC be up to 0.052 an 0.027 in reflectance units, at green and red bands, respectively (table 1). The errors are

**Chien-Hui Liu**, Department of Digital Media and Product Design, Transworld University, Douliu, Taiwan, R.O.C

computed from the means errors of the whole image. Corresponding relative errors are 64% and 32%, respectively.

The error at red band is reduced compared with green band (Fig. 3), because scattering is reduced as wavelength is increased (table 1). This is also shown in Fig. 4. Atmospheric effect is mainly dominated by water absorption at NIR and SWIR bands [3]. The reflectance errors, if AC is not concerned, are -0.011 (-5%) and -0.003 (-2%), at NIR and SWIR bands, respectively. These errors are much lower than those at visible bands (table 1). Unlike errors at visible bands, reflectance error due to AC neglection is different for various targets at NIR (Fig. 5). The error is positive on water pond targets, around zero for urban targets and negative for vegetation. This is because of the atmospheric absorption due to water vapor. The error is around zero at SWIR (Fig. 6), because water vapor absorption is lower as compared to that at NIR.

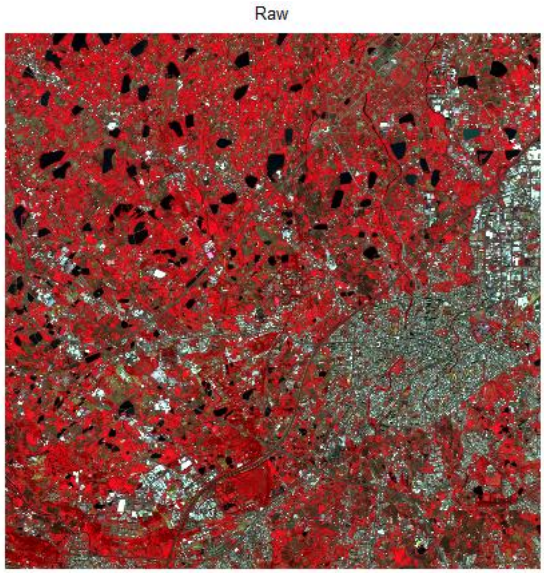


Fig. 1 SPOT satellite image over Taoyuan test site with false-color band combinations: near infrared (red), red (green) and green (blue). Image is taken on 2010/03/11.

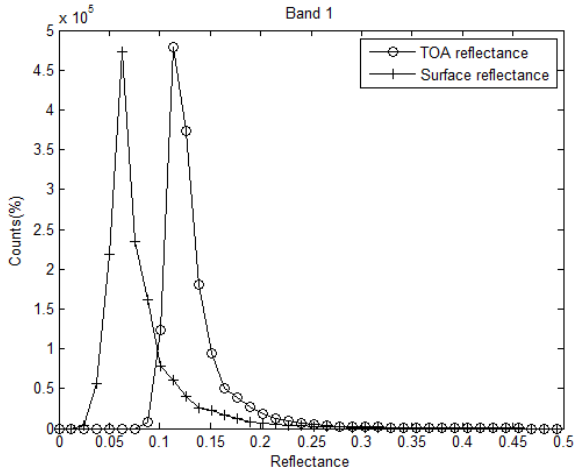


Fig. 2 Histogram of TOA reflectance and surface reflectance at green band

Table 1. Mean reflectances of TOA and surface of the whole image as well as error and relative error (%) at multiple bands.

| Bands | TOA | Surface | Err. | Rel. Err.(%) |
|---|---|---|---|---|
| Green | 0.133 | 0.081 | 0.052 | 64 |
| Red | 0.113 | 0.085 | 0.027 | 32 |
| NIR | 0.220 | 0.232 | -0.011 | -5 |
| SWIR | 0.175 | 0.178 | -0.003 | -2 |

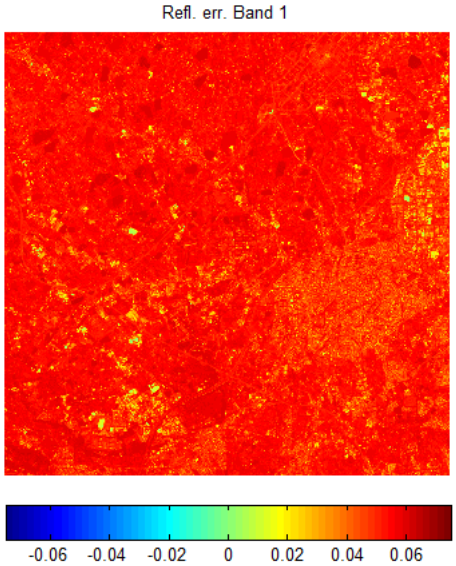


Fig. 3 Reflectance error due to AC at green band.

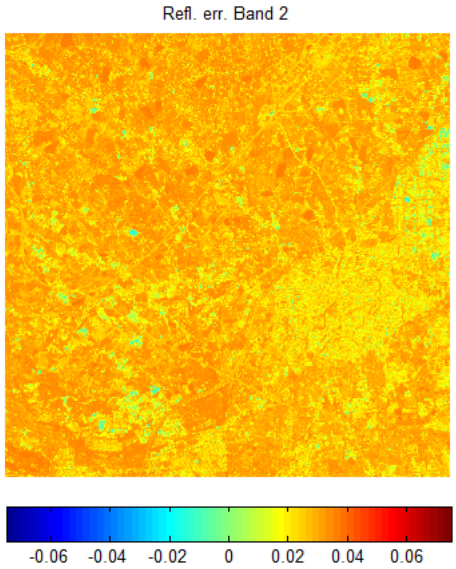


Fig. 4 Similar to Fig. 3, except at red band.

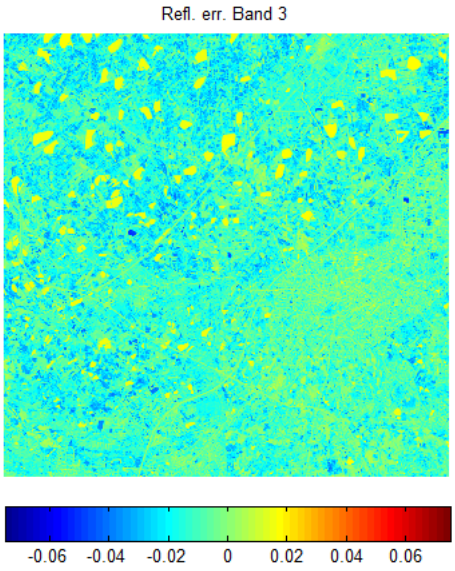


Fig. 5 Similar to Fig. 3, except at NIR band.

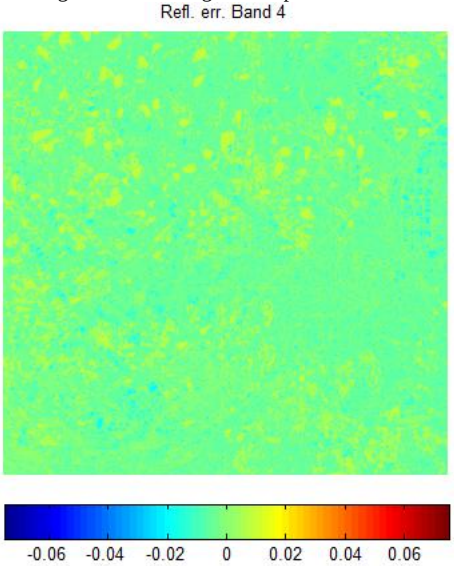


Fig. 6 Similar to Fig. 3, except at SWIR band.

## IV. Conclusion

In this study, the atmospheric correction algorithm of SPOT satellite image is introduced. Analysis of AE and physical mechanism of AE at different bands are performed. The results show that the importance of AC, especially at visible bands. Relative errors of reflectance, if AC is not concerned, are 64% and 32% at green and red bands, respectively. Currently, the algorithm is confined to cloudless images with uniform atmospheric effect. AC suitable for non-uniform AE will be improved in future.

## References

[1] Y. J. Kaufman, "Atmospheric effects on remote sensing of surface reflectance," *Remote Sens. Crit. Rev. Technol.*, vol. 475, pp. 20–33, 1984.
[2] Y. J. Kaufman and C. Sendra, "Algorithm for automatic atmospheric corrections to visible and near-IR satellite imagery," *Int. J. Remote Sens.*, vol. 9, no. 8, pp. 1357–1381, 1988.
[3] K.-N. Liou, *An introduction to atmospheric radiation*, vol. 84. Elsevier, 2002.
[4] R. Richter, "A spatially adaptive fast atmospheric correction algorithm," *Int. J. Remote Sens.*, vol. 17, no. 6, pp. 1201–1214, 1996.
[5] Y. J. Kaufman, D. Tanré, L. Remer, E. Vermote, A. Chu, and B. N. Holben, "Remote sensing of tropospheric aerosol from EOS-MODIS over the land using dark targets and dynamic aerosol models," *J Geophys Res*, vol. 102, pp. 17051–17067, 1997.
[6] V. Sharma, S. Ghosh, M. Bilal, S. Dey, and S. Singh, "Performance of MODIS C6. 1 dark target and deep blue aerosol products in Delhi national capital region, India: application for aerosol studies," *Atmospheric Pollut. Res.*, vol. 12, no. 3, pp. 65–74, 2021.
[7] D. G. Hadjimitsis, C. R. Clayton, and A. Retalis, "On the darkest pixel atmospheric correction algorithm: a revised procedure applied over satellite remotely sensed images intended for environmental applications," in *Remote Sensing for Environmental Monitoring, GIS Applications, and Geology III*, 2004, vol. 5239, pp. 464–471.
[8] Z. Zhang, G. He, and X. Wang, "A practical DOS model-based atmospheric correction algorithm," *Int. J. Remote Sens.*, vol. 31, no. 11, pp. 2837–2852, 2010.
[9] P. M. Teillet and G. Fedosejevs, "On the dark target approach to atmospheric correction of remotely sensed data," *Can. J. Remote Sens.*, vol. 21, no. 4, pp. 374–387, 1995.
[10] P. S. Chavez Jr, "An improved dark-object subtraction technique for atmospheric scattering correction of multispectral data," *Remote Sens. Environ.*, vol. 24, no. 3, pp. 459–479, 1988.
[11] S. Liang, H. Fallah-Adl, S. Kalluri, J. JáJá, Y. J. Kaufman, and J. R. Townshend, "An operational atmospheric correction algorithm for Landsat Thematic Mapper imagery over the land," *J. Geophys. Res. Atmospheres*, vol. 102, no. D14, pp. 17173–17186, 1997.
[12] H. Ouaidrari and E. F. Vermote, "Operational atmospheric correction of Landsat TM data," *Remote Sens. Environ.*, vol. 70, no. 1, pp. 4–15, 1999.
[13] Q. Vanhellemont, "Adaptation of the dark spectrum fitting atmospheric correction for aquatic applications of the Landsat and Sentinel-2 archives," *Remote Sens. Environ.*, vol. 225, pp. 175–192, 2019.
[14] A. Chudnovsky, A. Lyapustin, Y. Wang, C. Tang, J. Schwartz, and P. Koutrakis, "High resolution aerosol data from MODIS satellite for urban air quality studies," *Cent. Eur. J. Geosci.*, vol. 6, no. 1, pp. 17–26, 2014.
[15] A. Misra, "Validation of Version 5.1 MODIS Aerosol Optical Depth (Deep Blue Algorithm and Dark Target Approach) over a Semi-Arid Location in Western India," *Aerosol Air Qual. Res.*, 2015, doi: 10.4209/aaqr.2014.01.0004.
[16] C. Chen *et al.*, "Prototyping of LAI and FPAR retrievals from MODIS multi-angle implementation of atmospheric correction (MAIAC) data," *Remote Sens.*, vol. 9, no. 4, p. 370, 2017.
[17] S. Y. Kotchenova, E. F. Vermote, R. Matarrese, and F. J. Klemm Jr, "Validation of a vector version of the 6S radiative transfer code for atmospheric correction of satellite data. Part I: Path radiance," *Appl. Opt.*, vol. 45, no. 26, pp. 6762–6774, 2006.
[18] C.-H. Liu, "Normalized Difference Vegetation Index with Atmospheric Correction for Satellite Images," *Int. J. New Technol. Res.*, vol. 8, no. 5, pp. 14–16, 2022.